

Full Waveform Inversion

3D FWI of shallow seismic 9C wavefields

Thomas Bohlen



Agenda

1. Introduction
2. 3D 9C data acquisition
3. Initial model
4. 3D inversion results
5. Conclusions

Agenda

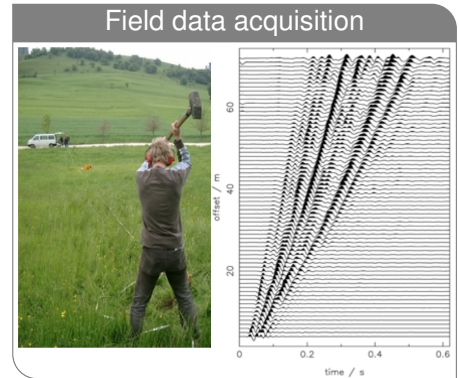
1. Introduction
2. 3D 9C data acquisition
3. Initial model
4. 3D inversion results
5. Conclusions

FWI for near surface characterization

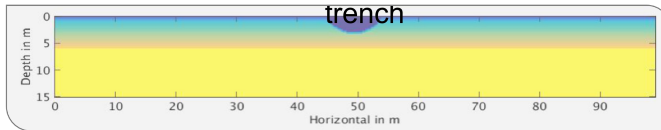
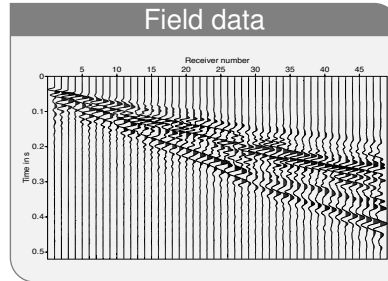
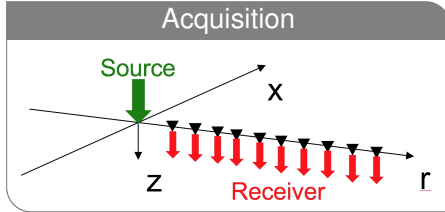
Shallow seismic surface waves are useful for geotechnical site characterization

- easily excited by a hammer blow
- surface waves are strong signals
- highly sensitive for **S-wave velocity**
- depth of investigation up to 10-15 m

FWI of surface waves is especially useful to infer small-scale lateral variations of V_s . The potential in recovering V_p , V_s , Q_p , Q_s , ρ must be investigated.

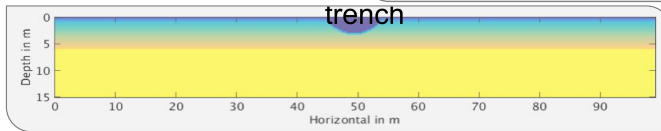
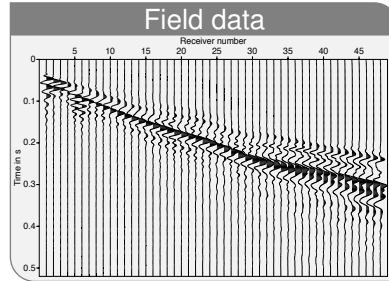
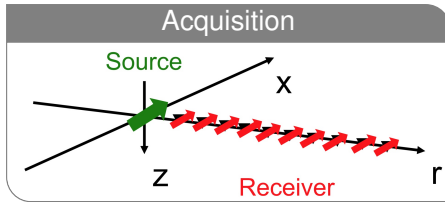


Reminder: 2D FWI of Rayleigh waves



Source and receiver in-line (x,z), 2D elastic FWI (P-SV wave equation) gives 2D models of $V_S(x, z)$

Reminder: 2D FWI of Love waves



Source and receiver cross-line (y); 2D elastic FWI (SH wave equation) gives 2D models of $V_S(x, z)$, independent of Rayleigh waves in 2D

Why 3D 9C FWI of shallow seismic wave fields ?

2D vs. 3D FWI

- 2D elastic FWI yields reliable 2D models of $V_s(x, z)$ beneath the profile.
- 2D assumption may fail in the presence of strong 3D lateral variations in V_s . This is most likely the case for the EL.
- High data redundancy in 3D 9C acquisition may improve 3D multi-parameter reconstruction.

Research questions (some)

- 1 Reconstruction of 3D models of V_s from multi-component data feasible ?
- 2 What is the optimal 9C acquisition configuration (data redundancy)
- 3 Strategy to quantify uncertainties (ROWI) - next lecture

Agenda

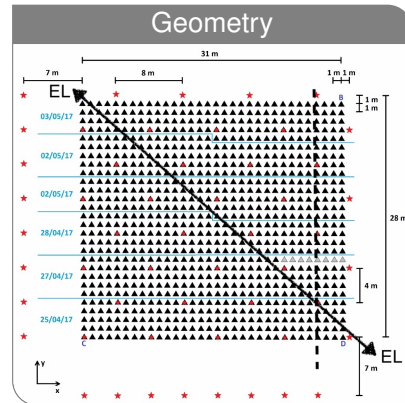
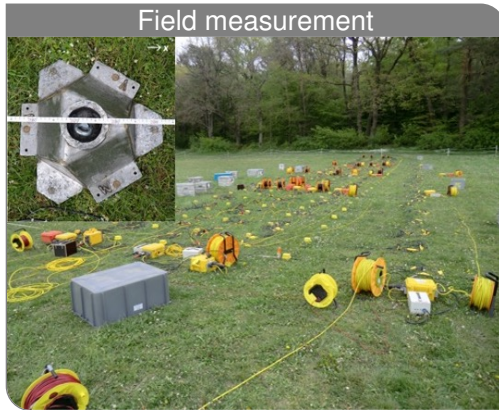
1. Introduction
2. 3D 9C data acquisition
3. Initial model
4. 3D inversion results
5. Conclusions

Field laboratory glider field Rheinstetten



Well defined trench "Ettlinger Linie" excavated in the 18th century: 5m wide and 2m deep.

3D 9C Acquisition 2017

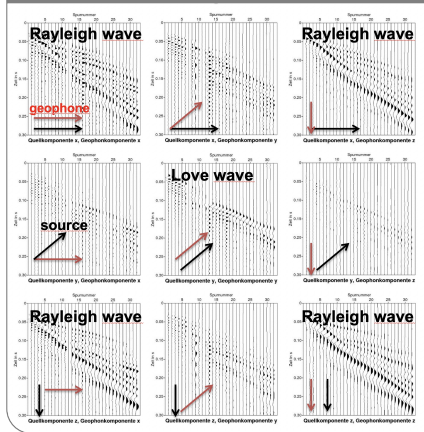


Area 31m x 27 m, 52 3-C Galpherin source locations ("UVW"), 896 3-C geophones (4.5 Hz, "XYZ"), 6 days, repetition of all source positions for each geophone patch

(Schaneng 2017)

Field data

Raw field data after wave source rotation

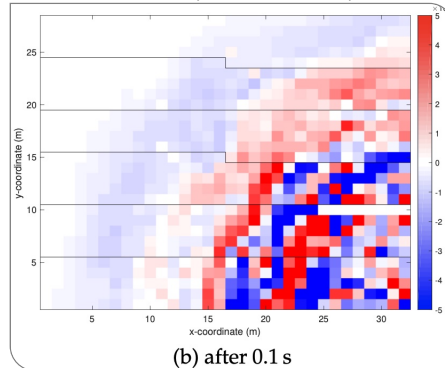


Data redundancy

- Rayleigh- and Love waves
- Rayleigh waves: 4C
- Cross-components show 3D effects

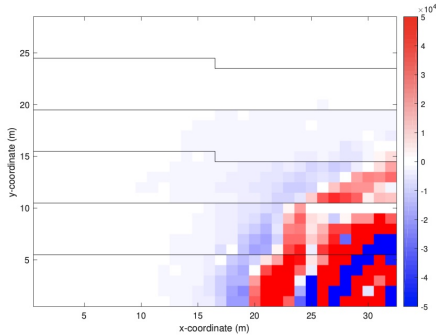
Movie of recorded wavefield

Source location 14, source component v, receiver component Z, Movie:

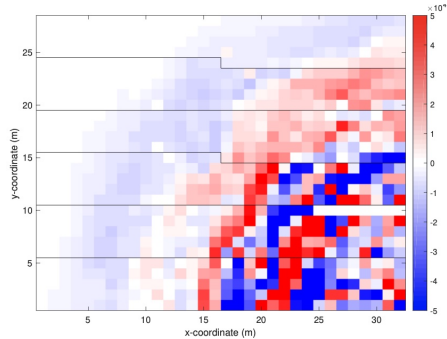


(Wienoebst 2020)

Recorded wavefield; Source v, Receiver Z



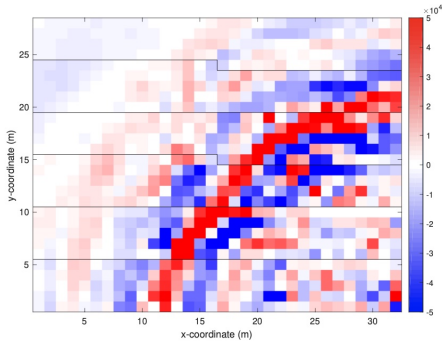
(a) after 0.05 s



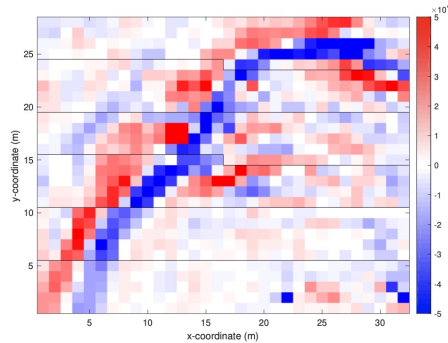
(b) after 0.1 s

(Wienoebst 2020)

Recorded wavefield; Source v, Receiver Z



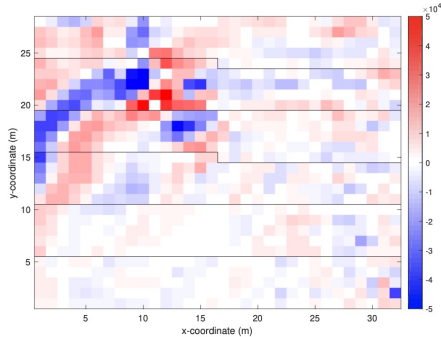
(c) after 0.15 s



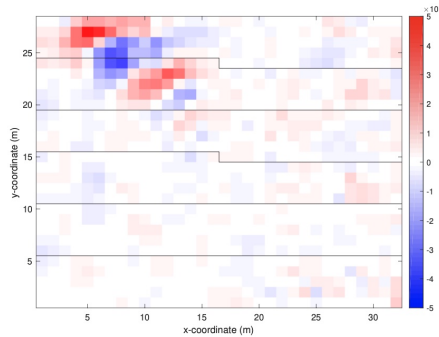
(d) after 0.2 s

(Wienoebst 2020)

Recorded wavefield; Source v, Receiver Z



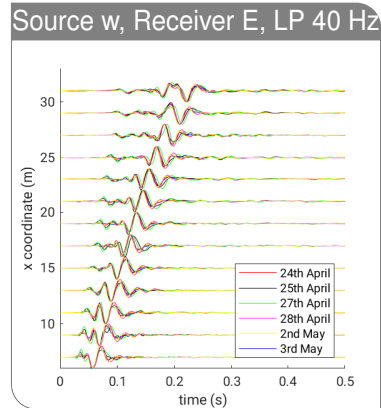
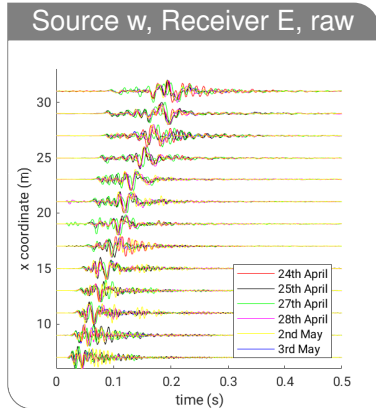
(e) after 0.25 s



(f) after 0.3 s

(Wienoebst 2020)

Daily variations at higher frequencies



(Wienoebst 2020)

Characteristics of 3D wave field

Wavefield characteristics

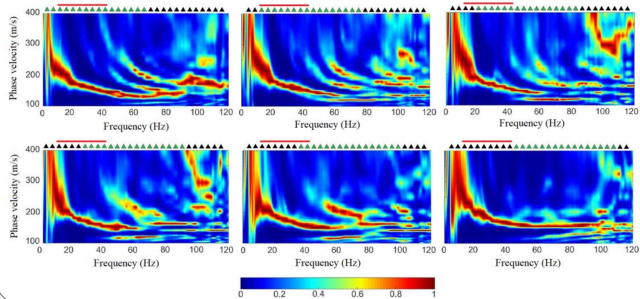
- Data consistent below approx. 40 Hz
- High amplitude surface waves
- Low amplitude fast refracted P-waves
- EL visible as low-velocity zone (delay of surface waves, amplitude focussing)

Agenda

1. Introduction
2. 3D 9C data acquisition
3. Initial model
4. 3D inversion results
5. Conclusions

Initial model by inversion of local dispersion curves

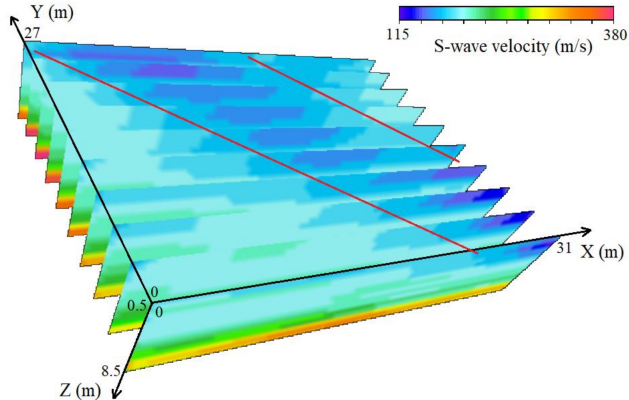
Local dispersion curves at $X=28\text{m}$, min. offset 7m



- Receivers in green are used in dispersion analysis
- Red line represents EL
- Note the variation of dispersion along the line
- Inverted 1D model is assigned to the center of the active receivers spread

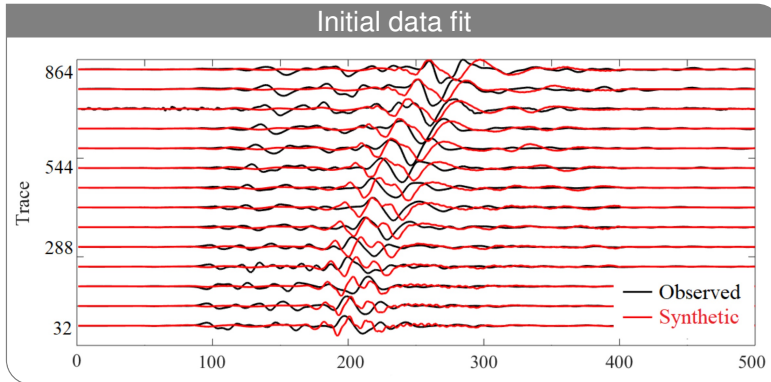
(Pan et al. 2018)

3D initial model of V_s



(Pan et al. 2018)

Initial data fit: no cycle skipping of surface waves



Agenda

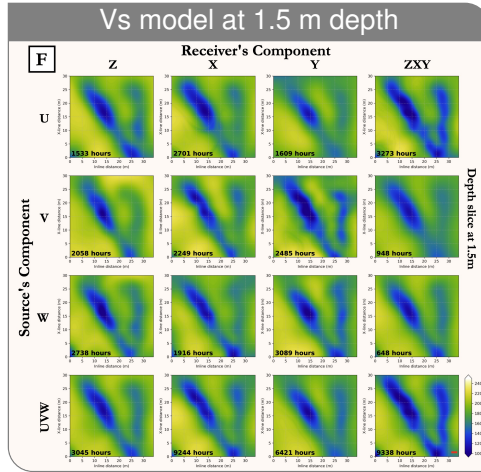
1. Introduction
2. 3D 9C data acquisition
3. Initial model
4. 3D inversion results
5. Conclusions

3D 9C elastic FWI - workflow

3D FWI Workflow

- Spectral element forward solver SEM46 (Trinh et al. 2019)
- Multi-scale 3-45 Hz
- Monoparameter V_s only, fixed V_s - V_p , V_s - ρ relations
- FWI performed in Grenoble (Irnaka et al. 2021)

3D 9C elastic FWI - final models



FWI results

- 2 distinct LVZs become visible
- Recording with 3C receiver components (X,Y, Z) seem to improve resolution and sharpen the image (full wave field recording is beneficial)
- 3C source (UVW) does not improve the reconstruction significantly (no additional excitation of waves by 3C sources)

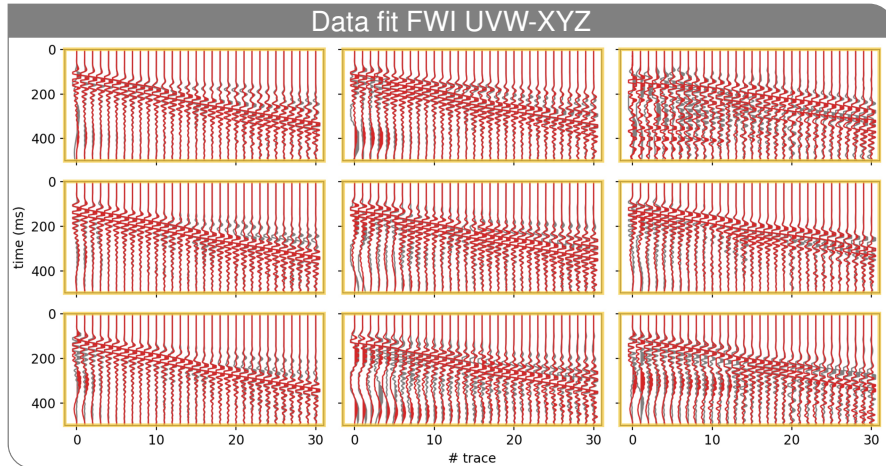
Sufficient data fit for all 9C combinations



→ data fit alone is not sufficient to assess the performance of different 9C configurations

(Irnaka et al., 2021)

Data fit for UVW-XYZ (full data set)



(Irnaka et al. 2021)

Agenda

1. Introduction
2. 3D 9C data acquisition
3. Initial model
4. 3D inversion results
5. Conclusions

3D FWI of 9C shallow seismic field data

Conclusions

- Initial models can be derived by the inversion of local dispersion curves
- 3D 9C elastic FWI is feasible with moderate computational efforts
- 3D models of V_S can be recovered reliably with high resolution
- 3C recording seem to be more important than 3C source excitation
- 9C FWI (full data set) enhances anomalies

Thank you for your attention

 Thomas.Bohlen@kit.edu
 <http://www.gpi.kit.edu/>

Published under  license.

References

- Irnaka, T. M., Brossier, R., Métivier, L., Bohlen, T. & Pan, Y. (2021), '3D Multi-component Full Waveform Inversion for Shallow-Seismic Target: Ettlingen Line Case Study', *Geophysical Journal International* . ggab512.
URL: <https://doi.org/10.1093/gji/ggab512>
- Pan, Y., Schaneng, S., Steinweg, T. & Bohlen, T. (2018), 'Estimating S-wave velocities from 3D 9-component shallow seismic data using local Rayleigh-wave dispersion curves – A field study', *Journal of Applied Geophysics* **159**, 532 – 539.
URL: <http://www.sciencedirect.com/science/article/pii/S0926985118306475>
- Schaneng, S. P. (2017), Erstellung eines 3D Modells der Scherwellengeschwindigkeit im Bereich der Ettlinger Linie (Rheinstetten) aus der 1D Inversion der lokalen Dispersion von Rayleigh-Wellen, Master's thesis, Karlsruher Institut für Technologie (KIT).
URL: <https://publikationen.bibliothek.kit.edu/1000080199>
- Trinh, P.-T., Brossier, R., Métivier, L., Tavard, L. & Virieux, J. (2019), 'Efficient time-domain 3D elastic and viscoelastic full-waveform inversion using a spectral-element method on flexible Cartesian-based mesh', *GEOPHYSICS* **84**(1), R61–R83.
URL: <https://doi.org/10.1190/geo2018-0059.1>
- Wienoebst, M. (2020), Towards 3D elastic full-waveform inversion of 9C shallow seismic Rheinstetten field data, Master's thesis, Karlsruher Institut für Technologie (KIT).
URL: <https://bwsyncandshare.kit.edu/s/XaENnPBTRASRoqC>